AERODYNAMIC SHAPE OPTIMIZATION OF BLENDED WING BODY PLANFORM

Hem Raj Pandeya [a], Anurag Karki [b], Sudip Bhattarai [c]

[a, b, c] *Department of Mechanical and Aerospace Engineering, Pulchowk Campus, IOE, Tribhuvan University, Nepal*
[e] sudip@ioe.edu.np

Abstract
The present research focuses on optimizing the lift/drag ratio of the existing Blended Wing Body (BWB) model 'Eagle Ray-baseline 3' through adjustments to key shape parameters—twist, dihedral, and sweep. Gradient-based optimization was performed in SU2 using the adjoint algorithm, leading to a 6% lift/drag ratio increment. Again, the same baseline was optimized using a non-gradient-based solver, Aeolus, and a 23% lift/drag ratio increment was obtained. Finally, some manual modifications were made based on literature, usability, and expert feedback, resulting in a 3% lift/drag ratio increment. CFD analysis of the baseline model and optimized models were done in ANSYS Fluent, and various parameters were analyzed. This research underscores the potential for significant performance gains from the synergy between advanced optimization methods and judicious manual refinements.

Keywords
Optmization, BWB, SU2, Aeolus, Adjoint, BOBYQA

1. Introduction

The Blended Wing Body (BWB) design is viewed as a potential breakthrough innovation in modern aviation. Unlike traditional aircraft design that features distinct components such as wings, fuselage, and tail, a blended wing body seamlessly integrates these elements into a single, cohesive body. This results in a unique and unconventional appearance, often characterized by smooth, curved surfaces that smoothly transition between different aircraft sections. In contrast to the conventional tube-and-wing configuration, the BWB exhibits exceptional aerodynamic performance [1, 2, 3], which arises from several factors: a significant reduction in the wetted area effectively minimizes skin friction drag, an all-lifting design lowers wing loading and enhances the distribution of lift along the wingspan, the seamlessly blended wing-center body junction diminishes interference drag, and the BWB's area-ruled shape mitigates wave drag, particularly at high transonic speeds.

Aside from improved efficiency and maneuverability [4], the BWB design is an excellent choice for UAVs. It is well-suited for integrating innovative technologies like advanced materials, artificial intelligence, and autonomous flight systems. This is possible mainly due to increased payload capacity due to a significant reduction in fuel consumption, leading to reduced direct operating costs [5,6].

Eagle Ray is a medium-sized BWB drone with an approximate weight of 20 kilograms designed to fly at high altitudes in the Himalayas in Nepal to protect endangered snow leopards, which are hunted for their coats and body parts [7]. For this mission in the Himalayas, the vehicle needs to have high efficiency, endurance, and better control. Discernibly, the endurance and range of an aircraft also depend upon the lift-to-drag ratio (E). Although UAV stability and control are paramount for the safe and precise operation of a UAV [8], this can be obtained by integrating various flight control systems that encompass both hardware and software components [9]. So, the prime focus in the optimization of the UAV will be on maximizing aerodynamic efficiency. As aerodynamic efficiency is directly influenced by the aircraft's shape, we will investigate various approaches for optimizing the aircraft's shape.

Figure 1: Eagle Ray

Now, reflecting on the history of aerodynamic shape optimization (ASO), significant progress occurred when flow solvers were integrated with optimization algorithms. However, a significant breakthrough in the evolution of aerodynamic optimization techniques took place in the late 1980s when Jameson and other researchers first applied adjoint methods [10, 11, 12] to problems defined by systems of partial differential equations. Adjoint methods represented a notable advancement as they enabled the more efficient calculation of the gradient of the aerodynamic figure of merit concerning the design variables compared to traditional finite difference methods. Currently, SU2 [13, 14, 15] stands out as a promising optimization tool employing an adjoint-based approach for shape optimization. What sets it apart is its open-source nature and inherent

modularity, rendering it an ideal software solution for research in BWB aircraft optimization [16, 17, 18].

However, complex shapes are possessed by BWB aircraft, and it becomes apparent that challenges may be faced by gradient-based optimization when dealing with such intricate geometries. Additionally, one of the disadvantages of gradient-based methods is that a local extremum instead of a global one could be converged to by them [19]. In order to have more insights, the implementation of a non-gradient-based optimization method on the baseline model is desired, which can avoid local optimum and numerical noise. Nevertheless, a large number of parameter evaluations is required by many gradient-free optimization algorithms, such as Genetic algorithms [20,21], in order to converge. The cost of Genetic Algorithm methods seems very high for our case, so the BOBYQA algorithm, which is computationally cheaper, is chosen. The BOBYQA method is used for gradient-free optimization, and an iteratively created quadratic approximation of the objective function is employed by it [22]. Furthermore, an optimum solution can be converged to relatively quickly by it as quadratic models of the objective function are built and used to guide the search toward the optimum. More iterations and function evaluations may be required by many other non-gradient-based methods to achieve similar results.

2. Optimization Process

2.1 Initial Geometry

Table 1: Baseline Geometric Parameters

Parameters	Values
Total Wing Span	5.15 m
Projected Wing Span	4.67 m
Projected Wing Area	1.47 m^2
Root Chord	1.149 m
Aspect Ratio	17.46
Taper Ratio	23.94
Mean Aerodynamic Chord	0.502 m
Position of Centre of Gravity	0.586 m (from leading-edge)
Wing Loading	13.6 kg/m2

2.2 Objective Function

We maximize the lift/drag coefficient, denoted by ”E”, at the nominal cruise condition for the optimization studies. The FFD boxes can only move in the vertical direction (y-axis). So, the design variable for the objective function is displacement in the y-axis.

2.3 Optimization based on gradient technique using SU2

Optimization based on gradient technique using SU2:

1. Generation of the grid for a baseline geometry to determine the flow field characteristics
2. Obtaining computational fluid dynamics results of the BWB for a given boundary conditions
3. Generating free-form deformation boxes for design optimization interests
4. Evaluation of gradients for the flow field with adjoint flow solver
5. Deforming the former geometry according to calculated gradients
6. Obtaining the new objective function value with new geometry

The SU2 modules used in our study are:

1. SU2 CFD - for performing computational fluid dynamics
2. SU2 DEF – deform the shape and fluid domain under the defined control points
3. SU2 DOT – computes the gradient for changing the shape to get optimal results.

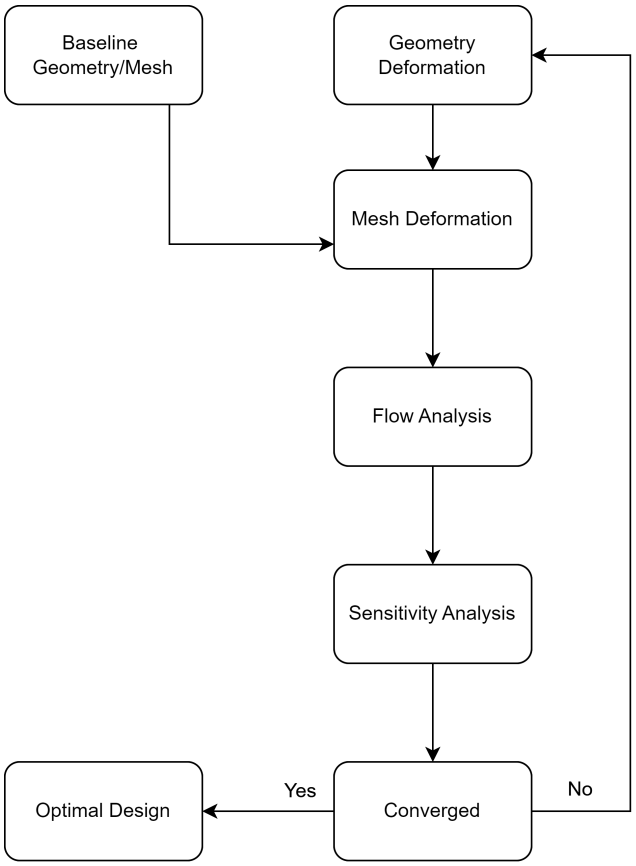

Figure 2: Flow Chart for gradient-based optimization within SU2

In the optimization approach, we employed a continuous adjoint-based solver to compute gradients. We initiated the process by defining control points in a script file, which led to the generation of a free-form deformation (FFD) box around the Blended Wing Body (BWB) model. The Reynolds-Averaged Navier-Stokes (RANS) model for computational fluid dynamics was utilized to iteratively deform the FFD box, surfaces, and volumes based on gradients calculated by the adjoint solver. This iterative process guided the optimization towards an optimal shape configuration, allowing us to enhance the performance of the BWB model.

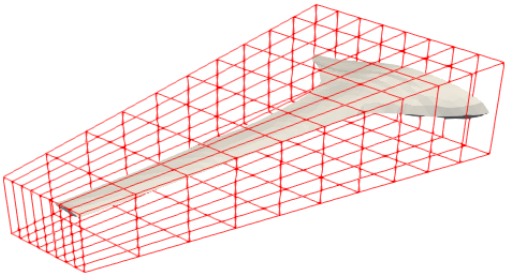

Figure 3: FFD box enclosing the Eagle Ray

Mesh for the optimization has been made in Ansys Mesh. It was converted to CGNS format, which can be read by SU2.

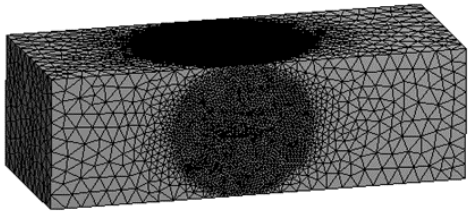

Figure 4: Mesh for optimization

Table 2: Baseline Geometric Parameters

Nodes	1653649
Elements	1219710

2.4 Optimizing with Aeolus: A Derivative-Free Approach

In mathematical optimization, non-gradient techniques have emerged to tackle scenarios where derivative information is scarce, unreliable, or impractical. This approach, known as derivative-free optimization, offers solutions in the absence of conventional derivatives. Aeolus employs the BOBYQA (Bound Optimization BY Quadratic Approximation) algorithm to optimize aircraft platforms. BOBYQA addresses optimization challenges within bound constraints without relying on objective function derivatives. Instead, it utilizes a trust region method, creating quadratic models through interpolation. Each iteration generates a new point, often through solving a trust region subproblem while respecting constraints. Alternatively, interpolation points can be replaced to enhance linearity.

Table 3: Parameters for Discretization

Parameter	Value
Number of panels per strip	48
Number of wing panels	6096
Number of strips	127
Mean panel aspect ratio	0.3
Panel distribution	Constant

Table 4: Flight Condition

Condition	Value
Weight	200 N
Fluid	Air
True Speed	20 m/s
Altitude	0 m
Density	1.22 Kg/m^3
Dynamic Pressure	5.488e+02 Pa

Table 5: Optimization Parameters

Parameter	Value
Algorithm	BOBYQA
Maximum iterations	1000
Objective function	lift/drag
Goal type	Maximize

3. Results and discussions

3.1 Results from SU2 optimization:

The effect of optimization can be seen in the aerodynamic parameters which can be visualized from the graphs below.

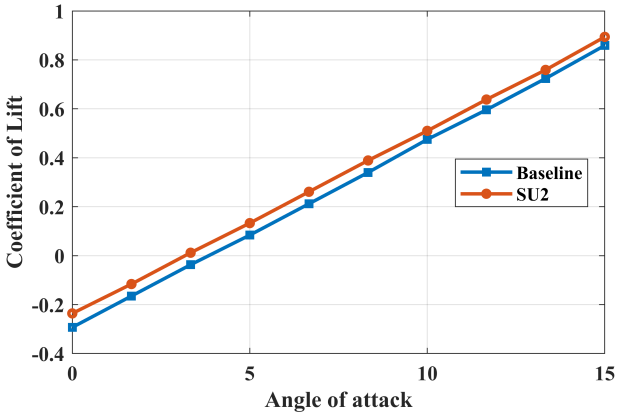

Figure 5: Plot showing C_L vs AoA

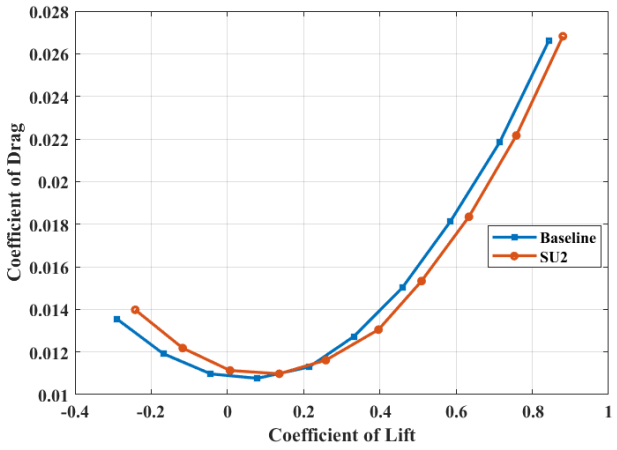

Figure 6: C_D vs C_L (C_D decreases by 5% at max cruise angle 10°)

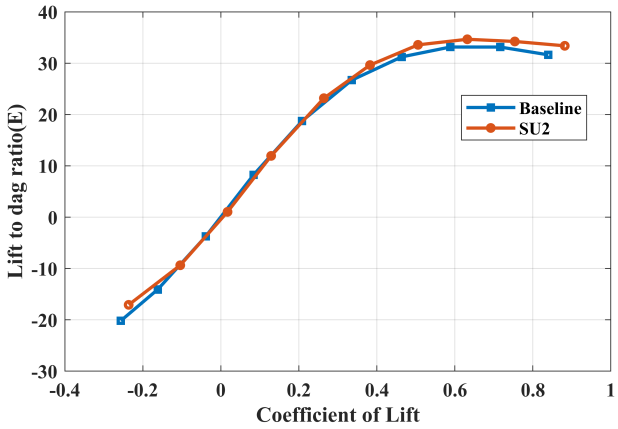

Figure 7: Graph of E vs C_L(6% rise in efficiency)

The above graphs show that using the gradient-based optimization, there is a tiny increment in the efficiency of the BWB planform. The lift/drag ratio is increased very little after crossing the Cl value of 0.5, i.e., nearly equal to a 10-degree angle of attack. The drag ratio is improved by 6% at a maximum angle of attack. Next, non-gradient bases optimization has been used to optimize the platform and further by changing the geometry manually.

3.2 Results from Aeolus optimization and manual modification:

After gradient-free optimization, DSN 4.1 was obtained, which underwent some manual changes based on literature reviews and usability considerations, leading to DSN 4.2.

DSN 4.1: Optimized Model (Sweep, Dihedral, and Twist): Our optimization process involves the wing with constrained winglets. We successively optimized for sweep, twist, and dihedral angles. While sweep and dihedral adjustments had minimal impact on the lift coefficient, variations in twist caused significant changes.

DSN 4.2: Model after Manual Modifications: We introduced minor changes for structural and manufacturing ease. Winglet sweep optimization decreased the sweep angle but increased vertical height. Adjustments in wingtip angle and maintaining washout smoothed integration with the center body. Shifting the wing forward maintained the desired center of gravity. These refinements led to DSN 4.2.

Our optimization journey encompassed meticulous adjustments to elevate aerodynamic efficiency and structural feasibility.

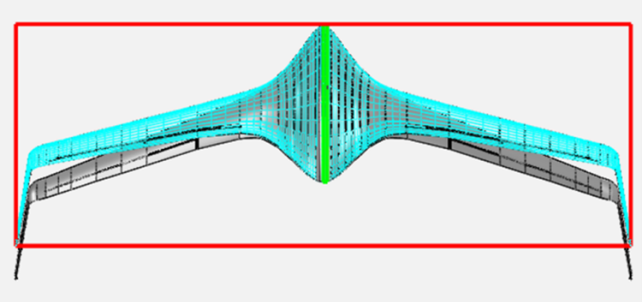

Figure 8: DSN 3(in Cyan) and DSN 4(in grey)

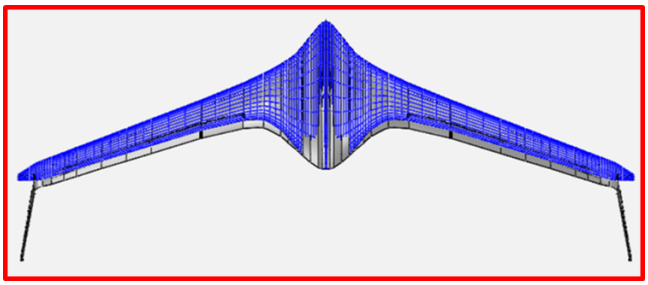

Figure 9: DSN 4.1 (in Grey) and DSN 4.2(in Blue)

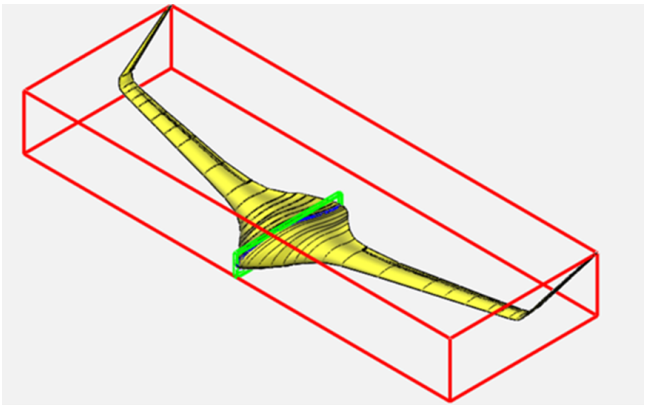

Figure 10: Isometric view of baseline model

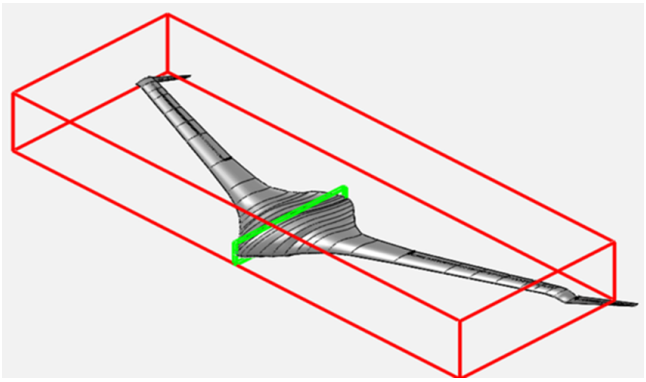

Figure 11: Isometric view of DSN 4.1

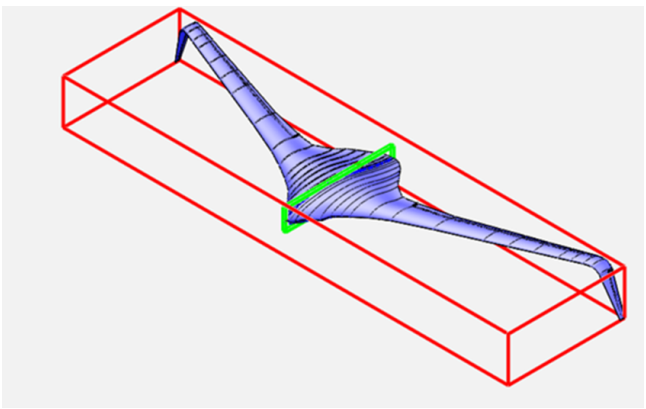

Figure 12: Isometric view of DSN 4.2 (reversed winglet)

In DSN 4.2 winglet is reversed for accommodation of landing gear.

Change in Performance Parameter:

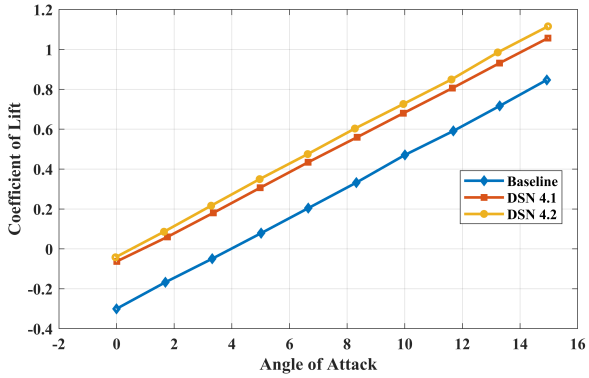

Figure 13: CL vs. AoA comparison in optimized models

The above graph shows that the value of CL is largely increased in DSN 4.1 and is slightly increased further in DSN 4.2.

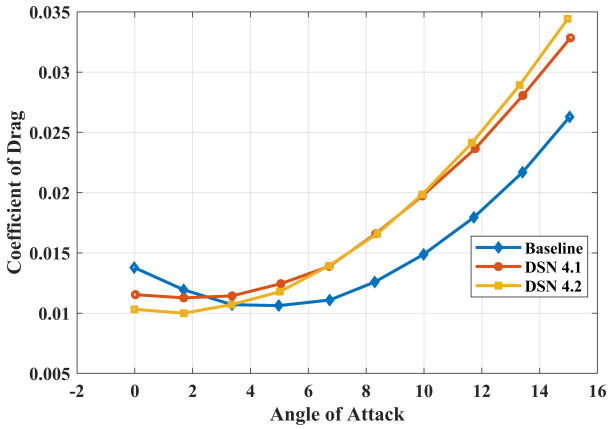

Figure 14: CD vs. AoA Comparison in Optimized Models

The drag force is shifted from 4 degrees to 1 in DSN 4.1 and DSN 4.2, which means the plane can be operated at a lower angle of attack.

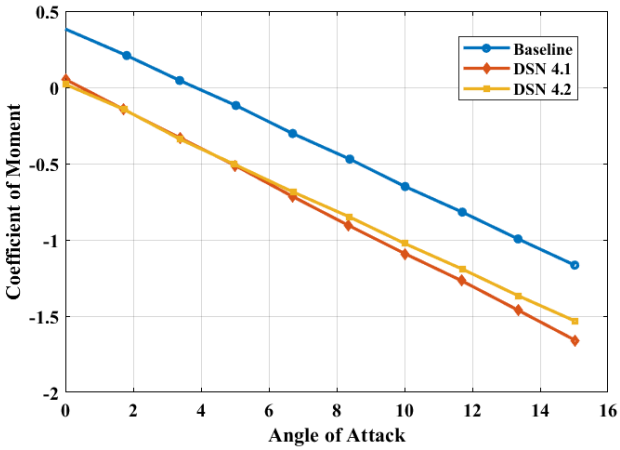

Figure 15: Cm vs AoA comparison in optimized models

After baseline 3 optimization, the zero-pitching moment is shifted from a 4-degree angle attack to a nearly zero-degree angle of attack. This helps to provide a more level flight.

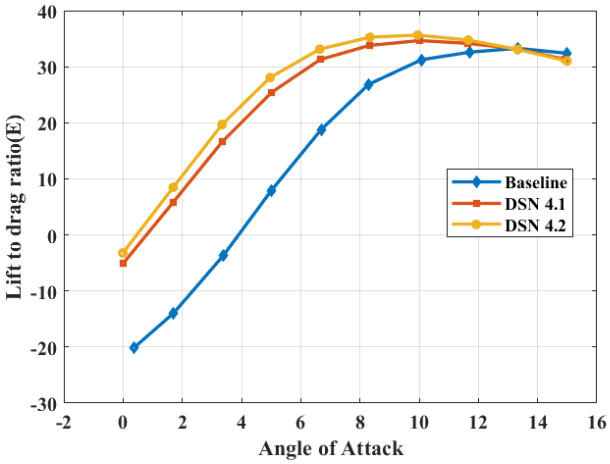

Figure 16: L/D vs AoA comparison for optimized models

After baseline 3 optimization, the value of CL/CD is largely increased which shows a high improvement in the performance of the vehicle. The value of CL/CD is further increased in DSN 4.2. The increase in lift-by-drag ratio was improved by 23% from baseline to DSN 4.1. Then after a few manual modifications, it was again improved by 3%.

4. Conclusion

The Initial Eagle Ray model, Baseline 3, was studied for different qualities. The baseline achieved a maximum lift-to-drag coefficient of 32 at a 10-degree angle of attack. It was also discovered that the model had a negative lift coefficient of -0.29046 when the angle of attack was zero degrees. The way the model behaved was shown in a moment diagram, indicating that the best angle of attack for balanced flight was about 4 degrees.

Improvements were made to the model in steps. Gradient-based optimization of the model was carried out using the Adjoint method in SU2, leading to a 6% increase in the lift-to-drag ratio.

Parallely, the initial model was optimized using a non-gradient-based algorithm, BOBYQA, in Aelous, giving rise to DSN 4.1, where changes were made to the design, like adjusting the sweep, dihedral, and twist angles. This resulted in a 23% boost in the lift-to-drag ratio.

More refinements were made to the model, including smoothing its shape and making minor adjustments based on feedback from experts and information from existing research. This created the model known as DSN 4.2, which brought an additional 3% improvement to the lift-to-drag ratio. In this version, the winglets were twisted downward to serve as support for the landing gear.

Furthermore, the model's shape now generates positive lift even at a zero-degree angle of attack. This also makes it easier to fly the aircraft at a lower angle of attack.

References

[1] R. H. Liebeck. Design of the blended wing body subsonic transport. *Journal of Aircraft*, 41(1), 2004.

[2] I. Kroo. Innovations in aeronautics. *American Institute of Aeronautics and Astronautics*, January 2004.

[3] N. Qin, A. Vavalle, A. Le Moigne, M. Laban, K. Hackett, and P. Weinerfelt. Aerodynamic considerations of blended wing body aircraft. *Progress in Aerospace Sciences*, 40(6), 2004.

[4] M. Voskuijl, G. La Rocca, and F. Dircken. Controllability of blended wing body aircraft. *International Council of the Aeronautical Sciences*, September 2008.

[5] R. Liebeck. Design of the blended wing body subsonic transport. *Journal of Aircraft*, 41(1), 2004.

[6] H. Smith. College of aeronautics blended wing body development programme. *International Council of the Aeronautical Sciences*, 114.1, 2000.

[7] Kashmir World Foundation. Eagle ray uas scans for poachers. `https://www.kashmirworldfoundation.org/post/eagle-ray-uas-scans-for-poachers`, August 26 2020.

[8] M. Baigang and W. Xiangyu. A new aerodynamic optimization method with the consideration of dynamic stability. *International Journal of Aerospace Engineering*, 2021, 2021.

[9] E. Ebeid, M. Skriver, and J. Jin. A survey on open-source flight control platforms of unmanned aerial vehicle. In *2017 Euromicro Conference on Digital System Design (DSD)*, pages 396–402, September 2017.

[10] A. Jameson. Aerodynamic design via control theory. *Journal of Scientific Computing*, 3, 1988.

[11] J. L. Lions. *Optimal control of systems governed by partial differential equations*, volume 170. Springer, 1971.

[12] O. Pironneau. On optimum design in fluid mechanics. *Journal of fluid mechanics*, 64(1), 1974.

[13] F. Palacios, M. R. Colonno, A. C. Aranake, A. Campos, S. R. Copeland, T. D. Economon, A. K. Lonkar, T. W. Lukaczyk, T. W. R. Taylor, and J. J. Alonso. Stanford university unstructured (su2): An open-source integrated computational environment for multi-physics simulation and design. In *51st AIAA Aerospace Sciences Meeting including the New Horizons Forum and Aerospace Exposition*. American Institute of Aeronautics and Astronautics, 2013.

[14] T. D. Economon, F. Palacios, S. R. Copeland, T. W. Lukaczyk, and J. J. Alonso. Su2: An open-source suite for multiphysics simulation and design. *AIAA Journal*, 54(3):828–846, 2016.

[15] F. Palacios, T. D. Economon, A. Aranake, S. R. Copeland, A. K. Lonkar, and [Additional Authors]. Stanford university unstructured (su2): Analysis and design technology for turbulent flows. In *52nd Aerospace Sciences Meeting*, 2014.

[16] S. Karpuk, Y. Liu, and A. Elham. Multi-fidelity design optimization of a long-range blended wing body aircraft with new airframe technologies. *Aerospace*, 7(7), 2020.

[17] Z. Lyu and J. R. Martins. Aerodynamic design optimization studies of a blended-wing-body aircraft. *Journal of Aircraft*, 51(5), 2014.

[18] G. Yang and A. Da Ronch. Aerodynamic shape optimisation of benchmark problems using su2. In *2018 AIAA/ASCE/AHS/ASC Structures, Structural Dynamics, and Materials Conference*. American Institute of Aeronautics and Astronautics.

[19] M. Lombardi, N. Parolini, A. Quarteroni, and G. Rozza. Numerical simulation of sailing boats: dynamics, fsi, and shape optimization. In *Variational Analysis and Aerospace Engineering: Mathematical Challenges for Aerospace Desig*. Springer US, 2012.

[20] A. Gara, M. A. Blumrich, D. Chen, G. L. T. Chiu, P. Coteus, M. E. Giampapa, and P. ... Vranas. Overview of the bluegene/l system architecture. *IBM Journal of Research and Development*, 54(5), 2010.

[21] D. E. Goldberg. *Genetic Algorithms in Search, Optimization, and Machine Learning*. Addison-Wesley, Reading, 1989.

[22] M.J.D. Powell. The bobyqa algorithm for bound-constrained optimization without derivatives. Technical report, Department of Applied Mathematics and Theoretical Physics, Cambridge, 2009.